

Angle of repose and segregation in cohesive granular matter

Azadeh Samadani and A. Kudrolli

Department of Physics, Clark University, Worcester, Massachusetts 01610

(Received 26 June 2001; published 16 October 2001)

We study the effect of fluids on the angle of repose and the segregation of granular matter poured into a silo. The experiments are conducted in two regimes where: (i) the volume fraction of the fluid (liquid) is small and it forms liquid bridges between particles thus giving rise to cohesive forces, and (ii) the particles are completely immersed in the fluid. The data is obtained by imaging the pile formed inside a quasi-two-dimensional silo through the transparent glass side walls and using color-coded particles. In the first series of experiments, the angle of repose is observed to increase sharply with the volume fraction of the fluid and then saturates at a value that depends on the size of the particles. We systematically study the effect of viscosity by using water-glycerol mixtures to vary it over at least three orders of magnitude while keeping the surface tension almost constant. Besides surface tension, the viscosity of the fluid is observed to have an effect on the angle of repose and the extent of segregation. In case of bidisperse particles, segregation is observed to decrease and finally saturate depending on the size ratio of the particles and the viscosity of the fluid. The sharp initial change and the subsequent saturation in the extent of segregation and angle of repose occurs over similar volume fraction of the fluid. Preferential clumping of small particles causes layering to occur when the size of the clumps of small particles exceeds the size of large particles. We calculate the azimuthal correlation function of particle density inside the pile to characterize the extent of layering. In the second series of experiments, particles are poured into a container filled with a fluid. Although the angle of repose is observed to be unchanged, segregation is observed to decrease with an increase in the viscosity of the fluid. The viscosity at which segregation decreases to zero depends on the size ratio of the particles.

DOI: 10.1103/PhysRevE.64.051301

PACS number(s): 45.70.Mg, 47.50.+d, 64.75.+g, 81.05.Rm

I. INTRODUCTION

The presence of small amounts of liquid can have a considerable influence on the properties of granular matter. For example, the angle of repose of a wet granular pile is greater than that of a dry pile made of the same material. Cohesive forces are introduced because of liquid bridges that are formed between particles. Cohesivity causes jamming in the flow of granular matter even in a regime where dry granular matter may flow. Wet granular matter is also observed to segregate less than dry granular matter as particles cannot move easily relative to each other. Although these qualitative facts are well known, a detailed knowledge of the properties even in comparison with dry granular matter has not yet been attained.

The properties of dry granular matter have attracted a considerable number of studies. Granular matter in a box that is tilted does not flow until a certain angle is exceeded at the surface. This angle, usually called the maximum angle of stability θ_m , depends on the frictional properties and the packing of the granular matter. However, if the granular matter is in motion, it may relax down to a lower angle that is called the angle of repose θ_r . The existence of the lower θ_r may be due to the lower kinetic friction compared to static friction between the particles and other dynamical effects [1]. The observed hysteresis may also occur because there are infinitely many metastable states above θ_r in which the system may get trapped [2].

In case of a very large pile of granular matter, it has been argued that θ_m is unaffected by the cohesivity introduced by the presence of the fluid. This is true provided that the frictional properties between the particles are unaltered due to

the presence of a lubrication layer. The basic argument is that while frictional force that helps hold a pile together increases with the size of the pile, the cohesive force is constant and becomes insignificant in comparison [3]. However, the effects may be important for a laboratory or industrial scale system. Recently, there have been a number of studies that have tried to relate the fluid content and its surface tension to observe increase in angles. θ_r measured by Hornbaker and collaborators [4,5] using the draining crater method is observed to initially increase linearly and then fluctuate around a constant value. For an ideal sphere-sphere contact, increasing the liquid content will lead to decreased cohesive force, and hence, a lowered θ_r . Therefore, they proposed that particle surface roughness plays an important role and a cone-plane type of contact between particles may be more appropriate. They also believed that the fluid coats the particles evenly. Mason *et al.* [6] have studied the distribution of the fluid on the surface of the particles using optical fluorescence microscopy and scanning electron microscopy. These studies appear to show that the fluid is in fact trapped in the menisci that are formed at the asperity on the grain surface. They have, therefore, claimed that the behavior of θ_m at low-volume fractions of the fluid is consistent with a scaling theory based on the surface roughness of the grains [7,8]. Other studies note that considerable differences between θ_r and θ_m may arise when humidity is present and have shown that the wetting properties of the fluid may be also important [9].

The identification of the occurrence and the extent of segregation is of considerable importance in material handling in industry. Preferential percolation of small particles through layers of larger particles is usually identified as lead-

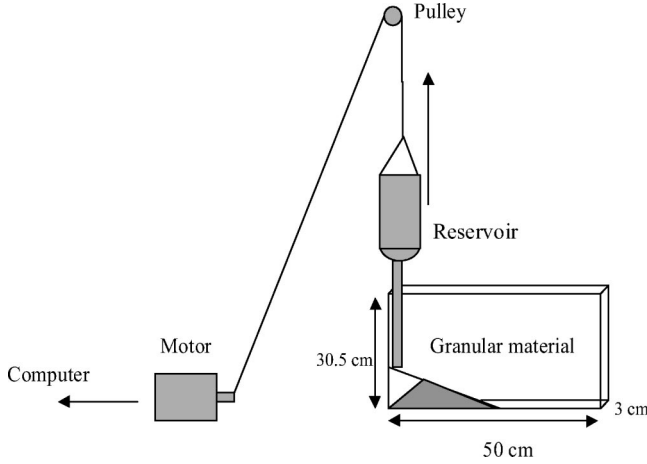


FIG. 1. Schematic diagram of the experimental setup. The reservoir containing the initial mixture is pulled up using a stepper motor in order to keep the height through which the mixture falls constant.

ing to segregation when granular flows occur at a free surface [10,11]. Stratification may occur in such systems if rough- and smooth-shaped grains are present [12]. The presence of the fluid alters the percolation of particles [13], and thus, has a profound influence on the progress of segregation in granular matter. It is, thus, surprising that the effects of the fluid on the progress of segregation has not been investigated in detail until recently. In a recent publication, we reported that the presence of a fluid drastically reduces segregation in bidisperse granular matter that is poured into a silo [14].

Although it is clear that the surface tension of the fluid is important in determining the cohesive force, and hence, θ_r , the role of the viscosity of the fluid ν may be less obvious. It is a common observation that a finger dipped in honey feels sticky in comparison to a finger dipped in water. This occurs because stronger forces are required to move the liquid into regions that are vacated. Therefore, viscous forces may have a significant effect on the dynamics of the grains. It is, thus, important to investigate the effect of ν on both θ_r and on size separation. Furthermore, viscous effects grow in importance for smaller dimensions. It may be possible to understand the effects of humidity on powders, which are smaller in size in comparison, by investigating effects of viscosity on segregation in granular systems [15]. This may be useful because quantitative studies with powders are more difficult to conduct.

In this context, we report a detailed study of the angle of repose and segregation of granular matter in the presence of a fluid using high-resolution digital imaging. Some of the results have been reported in a letter [14] and here we report additional data and analysis. We first investigate the effect of the size of the particles on θ_r as a function of the volume fraction of the fluid. We also discuss, in detail, our experimental observation of the effect of the viscosity ν of the fluid on θ_r . We then study the extent of segregation by visualizing the color-coded glass particles using bidisperse glass beads with size ratio r . Interestingly, the decrease in segregation is observed to saturate at similar values of volume fraction as θ_r . It may be also noted that small particles pref-

TABLE I. Monodisperse and bidisperse mixtures of spherical glass particles used in the experiment. d is the diameter of particles, r the size ratio, and θ_r the angle of repose of the dry particles.

Monodisperse	d (mm)	θ_r		
mono-1	0.1 ± 0.1	$23.5^\circ \pm 0.5^\circ$		
mono-2	0.5 ± 0.1	$24.0^\circ \pm 0.5^\circ$		
mono-3	0.9 ± 0.1	$24.0^\circ \pm 0.5^\circ$		
mono-4	1.2 ± 0.1	$24.0^\circ \pm 0.5^\circ$		
mono-5	3.1 ± 0.1	$25.5^\circ \pm 0.5^\circ$		
Bidisperse	d large	d small	r	θ_r
BD-1	mono-4	mono-3	1.3	$23^\circ \pm 0.5^\circ$
BD-2	mono-4	mono-2	2.4	$23^\circ \pm 0.5^\circ$
BD-3	mono-5	mono-2	6.2	$25^\circ \pm 0.5^\circ$
BD-4	mono-5	mono-1	31	$24^\circ \pm 0.5^\circ$

erentially clump in a bidisperse mixture and this leads to subtle effects on the nature of the particle spatial distribution as the volume fraction of the fluid is increased. As the volume fraction of the fluid increases and as the limit is approached where all the interstitial volume is saturated with the fluid, one may expect that the effects of the cohesion introduced by liquid bridges to become less important. This may have an effect on θ_r and size separation. However, there are practical difficulties in investigating high-volume fractions because the fluid tends to drain. Therefore, we also conducted experiments when the particles are completely immersed in a fluid to understand this limit.

II. EXPERIMENTAL APPARATUS

A schematic of the experimental apparatus is shown in Fig. 1. A rectangular silo of dimensions 50.0×30.5 cm and a width w of 3.0 cm is used for the experiments. The flow is visualized through the glass side walls of the silo using a 1000×1000 pixel Kodak ES 1.0 digital camera. The glass particles and fluids used are listed in Tables I and II, respectively. The granular sample is prepared in batches by

TABLE II. The fluids used in the experiments. ν is the viscosity, ρ the density, and Γ is the surface tension of the fluid. All data corresponds to 25°C except in case of polybutene H-300, where the lower ν is obtained by heating the tank to 50°C . Water-glycerol-1 and water-glycerol-2 contain 60% and 88% glycerol by weight, respectively [17].

Fluid	ν (N s m^{-2})	ρ (kg m^{-3})	Γ (Nm^{-1})
Water	0.0010	997	0.07 ± 0.003
Water-glycerol-1	0.0098	1076	0.07 ± 0.003
Water-glycerol-2	0.1190	1108	0.07 ± 0.003
Glycerol	1.5	1126	0.07 ± 0.003
Polybutene L-50	0.22	844	0.03 ± 0.003
Polybutene H-300	30	892	
Polybutene H-300	100	892	

thoroughly mixing 1.0 kilogram of each of the two kinds of particles with the fluid before the mixture is placed inside the reservoir. The volume fraction V_f of the fluid is calculated as the ratio of the volume of the fluid to the volume of all the particles. The volume of the particles corresponds to the weight of the particles divided by the density of the glass beads that is 2.4 g cm^{-3} .

The wet granular material is first filled into a reservoir and then drained through a pipe into the silo. In previous experiments, we demonstrated that segregation may occur during draining of a wide silo [16] and showed that size separation occurs in the surface flow regions. We also showed that segregation does not occur in the bulk by visualizing the flow. Therefore, by using a tall cylindrical reservoir, we minimize surface flow and prevent segregation from occurring during pouring. Pipes with various diameters are used to control the flow rate Q . Larger diameters are used at higher V_f in order to maintain $Q \sim 2.2 \text{ g s}^{-1}$. The reservoir is raised at a slow constant rate with a stepper motor and a system of pulleys. The slow upward velocity of the reservoir allows the particles to accumulate inside the pipe before flowing down the surface and reduces the kinetic energy of particles due to free fall. Such precautions are necessary, otherwise particles acquire substantial kinetic energy during free fall and tend to bounce back from the surface several times leading to size separation and stratification in the case of bidisperse particles. Smaller particles bounce back higher from the surface of the pile and land further down the pile in contrast to what is usually observed, i.e., small particles at the top of the sandpile. This effect, coupled with periodic avalanching observed at the surface, may lead to alternate layers of mixed and small particles. By using the pipe, we ensure that the interaction of particles is restricted to the surface of the pile. Thus, the number of mechanisms involved in segregation is reduced and the system is simpler.

We varied the time that the sample was mixed and found it had little effect on θ_r . We also waited a varying amount of time before pouring to test the effect of evaporation. We found that only in the case of water, there was a small influence if we waited for one hour for volume fractions below $V_f < 2 \times 10^{-3}$. Therefore, to minimize the effects of evaporation, the mixture was poured immediately after mixing.

III. THE EFFECT OF INTERSTITIAL FLUID ON THE ANGLE OF REPOSE

A triangular-shaped granular pile is formed after the material is poured into the silo. The flow of the granular material is continuous for dry particles, but becomes increasingly stick slip as V_f is increased. The flowing region is roughly 10 layers deep for dry particles, but the flow region becomes deeper and is not as well defined as V_f is increased. The resulting pile for monodisperse glass particles is shown in Fig. 2 and it may be observed that the surface of the wet pile is at a greater inclination than the dry pile.

A. Size dependence of the angle of repose

θ_r is measured by obtaining images of the sand pile after the silo is filled and fitting a straight line to the surface of the

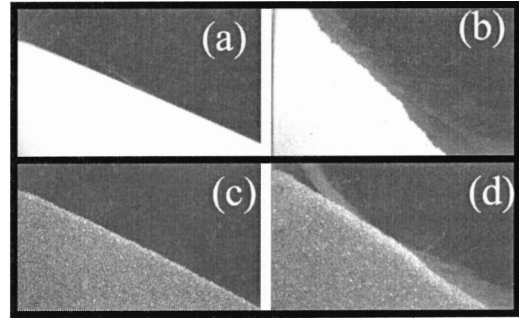


FIG. 2. Images of a pile of dry and wet monodisperse particles. (a) $V_f=0$, $d=0.5 \text{ mm}$, (b) $V_f=10^{-2}$, $d=0.5 \text{ mm}$, (c) $V_f=0$, $d=3.1 \text{ mm}$, (d) $V_f=10^{-2}$, $d=3.1 \text{ mm}$. θ_r is observed to be greater for the wet case and the surface of the pile of small particles is observed to be rough compared to the larger particles.

pile. The obtained slope is averaged over 10–15 images as a centimeter deep layer of granular matter is added and a new surface is created. θ_r is plotted as a function of V_f for particles with various diameters d in Fig. 3(a). θ_r is first observed to increase sharply with V_f and then saturate approximately. The value of V_f at which θ_r begins to saturate is V_c . The saturation value of θ_r is observed to increase with the size of the particles. This fact may be qualitatively noted from Fig. 2.

The increase and approximate saturation of θ_r is qualitatively similar to those earlier observed using the draining crater method [4,5]. Quantitative differences exist perhaps because of the difference in the geometries. As discussed in the introduction, both the increase in θ_r and saturation is surprising if one assumes ideal spheres in contact. To explain this property, work has focused on the fact that particles are not perfectly smooth but have asperities. Using the Mohr-Coloumb analysis and making assumptions for the height and distance over which the surface of the sphere fluctuates, Halsey and Levin [7] found that θ_m can increase linearly and then saturate to a value given by

$$\tan \theta_m \sim k + \frac{\sqrt{8} \pi k \Gamma}{d \rho_g g H} \sec[\tan^{-1}(k)], \quad (1)$$

where k is coefficient of static friction, Γ is the surface tension of the fluid, g is acceleration due to gravity, ρ_g is the density of the particles, and H is the height of the pile. It has been assumed here that the capillary force F_{cap} between the particles is given by $\pi \Gamma d$. They assume that the saturation will occur approximately when the wetting is determined by the macroscopic curvature of the particles, which is greater than the scale of the roughness of the surface of the particles. According to the model, volume V_c is given by $\lambda^2 d$ where λ is length scale over which fluctuations occur. The model predicts that θ_m decreases with d , which is consistent with our observations. Although there is a qualitative agreement between our data for θ_r and the model for θ_m [7], there is considerable disagreement related to the value of V_c . For example, for 1 mm particles, where the particle surface fluctuations are about $1 \text{ } \mu\text{m}$, the model predicts saturation for

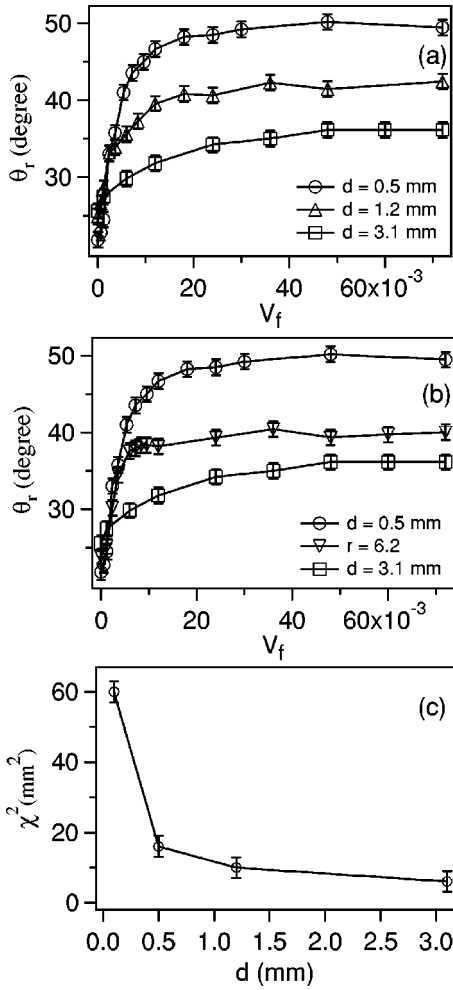


FIG. 3. (a) Size dependence of the θ_r for $d=0.5$ mm, $d=1.2$ mm, and $d=3.1$ mm glass beads. Note that θ_r is lower for larger d . (b) The saturation value of the θ_r of bimixtures are in between the θ_r of their components. (c) The mean square of the deviation of the surface from a straight line. The smaller particles are observed to stick together more readily, and make more clumps giving rise to a rougher surface and higher χ^2 .

$V_c \sim 10^{-5}$. However, the observed V_c is significantly higher and is approximately 5×10^{-3} .

While it is possible that the disagreement may arise because θ_m is calculated and θ_r is measured, additional effects may have to be taken into account in calculating the average cohesive force due to capillary bridges. For example, it has been assumed that only the capillary forces between particles in contact is important. However, it is possible that as V_f increases, particles that are slightly away from each other can also form liquid bridges. Therefore, it is possible that the average number of liquid bridges per particle increases with V_f . This effect may be important in determining the regime over which θ_r can increase.

We plot in Fig. 3(b), the θ_r for particles with $d=0.5$ mm and 3.1 mm and the bidisperse mixture (BD-3) to illustrate the behavior of θ_r when particles of different diameters are present. The θ_r for the bidisperse mixtures are located in between the θ_r of their components. A similar effect is observed for the other size ratios.

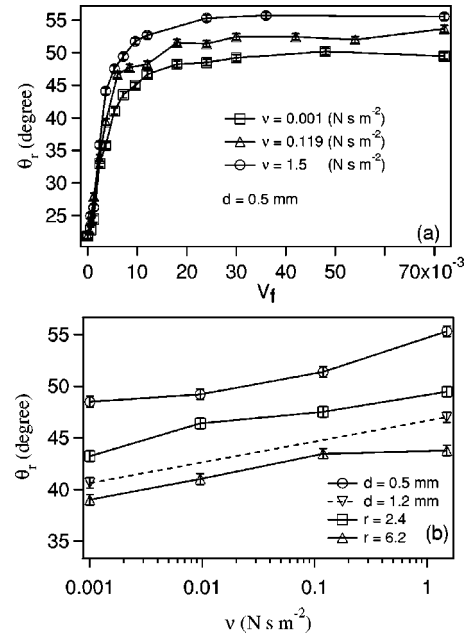


FIG. 4. (a) θ_r for monodisperse particles as a function of V_f , for water ($\nu=10^{-3}$ N s m^{-2}), glycerol ($\nu=1.5$ N s m^{-2}) and water-glycerol mixture ($\nu=0.12$ N s m^{-2}). (b) θ_r as a function of ν for different bimixture and monodisperse particles for $V_f=24 \times 10^{-3}$.

Besides the increase of θ_r due to the addition of the fluid, the surface of the pile is observed to become rough [see Figs. 2(b), 2(d)]. In addition, the roughness of the surface of the pile is greater for the smaller particles. We plot the mean square of the deviation of the surface from a straight line χ^2 for the particles mixed with water for a fixed $V_f=24 \times 10^{-3}$ in Fig. 3(c) to quantitatively show the increase in roughness with decreases in particle size. We observe that smaller particles clump more than larger particles at similar V_f . We therefore believe that the increased roughness of the surface is because of the clumping of the particles. As the particles form more clumps, the surface becomes increasingly rough and χ^2 grows. The standard deviation of θ_r obtained by repeating measurements for a particular V_f was reported in Ref. [5] as a measure of clumping. The reported observations are consistent with our more direct measurement of the surface heights. We will later see that the preferential clumping of small particles has an important effect on the progress of segregation and introduces layering.

B. Effect of viscosity of the fluid on the angle of repose

To investigate the effect of viscosity on the flow and the angle of repose, we kept the surface tension of the fluid constant and change ν of the fluid. Because water and glycerol have very similar surface tension, we used mixtures of these two fluids to change ν [17]. Glycerol dissolves in water and the mixture is homogenous after it is stirred for a few minutes. Using water-glycerol mixtures we obtained θ_r as a function of V_f .

In Fig. 4(a) we plot θ_r for $d=0.5$ mm beads as a function of V_f , for water, glycerol, and a water-glycerol mixture. Figure 4(a) shows that θ_r increases with ν . The increase is ob-

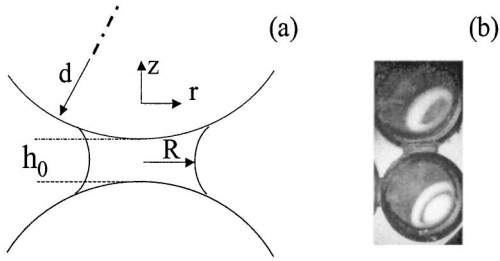


FIG. 5. (a) Schematic of a liquid bridge between two particles. (b) Image of a liquid bridge between two 0.1 mm particles corresponding to $V_f = 24 \times 10^{-3}$.

served to be sharper and the saturation is observed to occur at higher values for glycerol compared to water. We chose $V_f = 24 \times 10^{-3}$ in the saturated regime to plot θ_r as a function of ν for monodisperse particles and bidisperse mixtures in Fig. 4(b). We observe that the saturation value for θ_r depends on ν and increases with ν .

We have measured θ_r up to 48 hours after the granular mixture is poured into the silo. While a few local rearrangements occur up to a few minutes after pouring, we do not find measurable changes in the surface, thus indicating the absence of creep. We have thus shown that the viscosity of the fluid clearly influences the observed θ_r . In the next section, we will discuss the viscous force between the particles due to the fluid.

C. Estimates of the viscous force

Let us consider two particles that are moving away from each other. A schematic diagram is shown in Fig. 5(a). Figure 5(b) shows 0.1 mm particles mixed with glycerol for $V_f = 24 \times 10^{-3}$. Based on Reynolds lubrication theory, an expression for the viscous force has been derived for two identical rigid spherical surfaces [18–20]. The theory relates the pressure P generated in the liquid to the relative displacement of the two particles as

$$\frac{d}{dr_1} \left[r_1 H^3(r_1) \frac{dP(r_1)}{dr_1} \right] = 12\nu r_1 \frac{dh}{dt}, \quad (2)$$

where, $H(r_1) = h_0 + 2r_1^2/d$ is the distance between the two surfaces at radial distance r_1 from the center [see Fig. 5(a)]. If the particles are completely immersed in the fluid, the expression for the viscous force is

$$F_{vis} = -\frac{3}{8} \pi \nu d^2 \frac{1}{h_0} \frac{\partial h_0}{\partial t}. \quad (3)$$

For a liquid bridge, there is a correction coefficient [18] to Eq. (3) and the expression for the force is

$$F_{vis} = -\frac{3}{8} \pi \nu d^2 \left[1 - \frac{h_0}{H(R)} \right]^2 \frac{1}{h_0} \frac{\partial h_0}{\partial t}, \quad (4)$$

where R is the radius of the contact area. This equation may be related to the volume of the liquid bridge using $V = \int_0^R 2\pi r_1 H(r_1) dr_1$. Pitois *et al.* [18] experimentally investigated the effect of viscosity of the fluid on the properties of

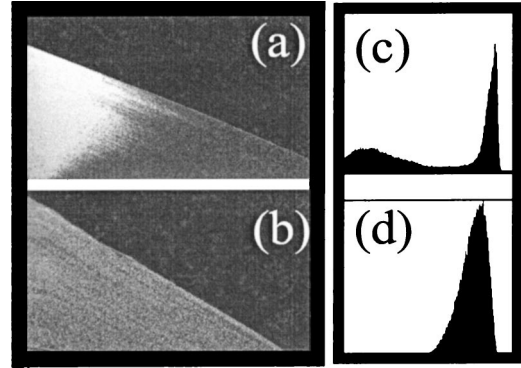


FIG. 6. Image of the granular pile after bidisperse glass beads are poured into the silo ($r=2.4$). The small particles are white and the large particles are black. (a) $V_f=0$, (b) $V_f=6 \times 10^{-3}$. Strong segregation is observed for the dry case, the segregation is drastically reduced when less than 1% of water is present in the mixture. (c)–(d) The histogram of local particle density ratio of the two kinds of particles in the pile. The peaks in the distribution can be fitted to Gaussian and the mean value used to determine the most common particle ratios.

a liquid bridge between two moving spheres. They showed that Eq. (4) fits their experimental data.

The value of the viscous force in our experiments may be estimated assuming that $\partial h_0 / \partial t$ is of the order of the velocity of the particles flowing down the surface. For 1 mm particles, if h_0 is of the order of 10 μm , then $F_{vis} \sim 10^{-7}$ N for water and $F_{vis} \sim 2 \times 10^{-4}$ N for glycerol. The capillary force estimated using $F_{cap} = \pi \Gamma d$ for 1 mm particles is 10^{-4} N. Therefore, the viscous force for glycerol is relevant, whereas for water, the viscous force may be insignificant. These improved results are also consistent with our previous estimates obtained neglecting the curvature of the particles [14].

Because viscous force decreases with relative velocity, it appears surprising that the viscosity of fluid plays any role at all in determining θ_r in our experiments and we return to this point later in the paper. However, it is clear that such forces are important in determining the extent of segregation as it occurs when the particles are in motion.

IV. EFFECT OF INTERSTITIAL FLUID ON SIZE SEGREGATION

To study the segregation of the particles in the pile, we use different colors for the two kinds of particles. Figure 6(a) shows a pile after dry bidisperse granular material has been poured inside the silo. Here, the small particles appear white and the large particles appear black. Thus, strong size separation is observed as the granular matter flow down the inclined surface. Two main mechanisms are important in determining the observed spatial distribution: (i) the void-filling mechanism where smaller particles percolate through the larger particles and are thus found at the bottom of the flow [11], and (ii) the capture mechanism where the smaller particles that are more sensitive to surface fluctuations are stopped at the top of the pile before the larger particles [21]. Segregation is observed to vanish when a small amount of

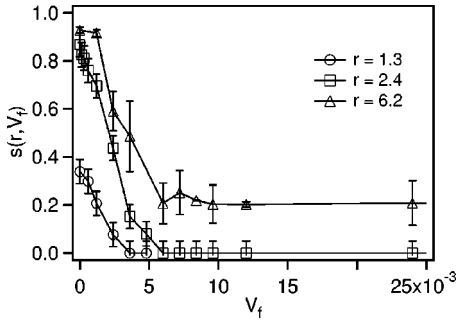


FIG. 7. The extent of segregation s observed in bidisperse particles as a function of V_f of water for various size ratios r . Segregation decreases and saturates, when V_f is greater than V_c . Segregation may persist if r is large.

fluid is added. Figure 6(b) shows the situation where $V_f = 6 \times 10^{-3}$, which corresponds to *less than 1%* by volume of water in the system. Thus, a very small amount of fluid is observed to prevent segregation from occurring.

To parametrize the extent of segregation, a histogram of the ratios of the two types of particles in a 3.5 mm^2 area is measured using the light intensity. The light intensity is a monotonic function of the density ratio of the particles and is measured by using pre-determined weight ratios of particles in a separate series of calibration experiments. The histogram of local particle density ratio P_w of the two kinds of particles in the pile is thus obtained and is plotted in Figs. 6(c), 6(d). The peaks in distribution may be fitted to a Gaussian and the mean value is used to determine the most common particle ratios a and b . The segregation parameter is defined as $s = (b - a)/100$ which has a value between 0 and 1 and describes the extent of segregation.

A. Dependence of the segregation on the size ratio

s for three different bidisperse granular mixtures BD-1, BD-2, BD-3, (see Table I) are plotted in Fig. 7(a) as a function of V_f of water. s depends on the size ratio r of particles, and goes to zero at lower V_f for smaller r . However, segregation may persist even in the presence of fluid although the extent is considerably smaller. A phase diagram of the observed segregation as a function of r and V_f may be found in Ref. [14].

B. Discussion of segregation on r size ratio

The observed properties may be described in terms of the differences in the strength of interactions between particles due to a difference in the sizes. In the presence of a wetting fluid, there are three possible interaction between the particles: interactions between the (i) small and small S - S particles, (ii) small and large S - L particles, and (iii) large and large L - L particles. In addition, the particles and clumps will also interact with the inclined surface on which they flow.

At small V_f , the fluid is observed to selectively coat the small particles forming clumps of small particles due to the cohesive forces discussed earlier. Most of these interactions are in the form of S - S interactions. There is less percolation of small particles through larger particles, thus reducing s .

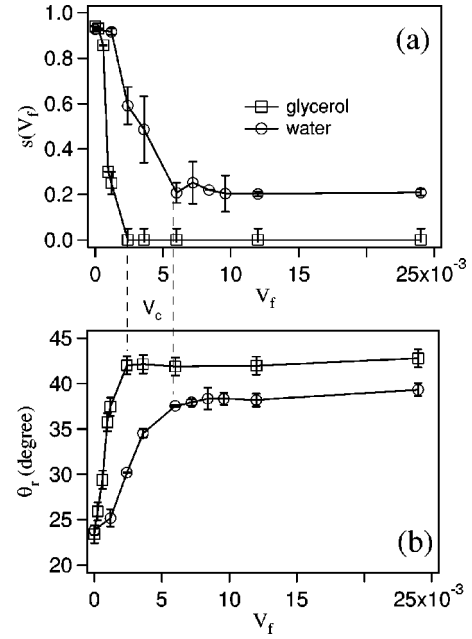


FIG. 8. Viscosity dependence of the s and θ_f for $r=6.2$ as a function of V_f . Note that the saturation value V_c is similar for s and θ .

By increasing the amount of fluid further, the size of clumps increases, the S - L interaction also become important, resulting in even smaller s . Finally, above a certain $V_f \sim V_c$, all types of interaction may be present, clumps are formed with both kinds of particles, and segregation saturates. For large r , clumps of S - L particles appear but are not strong enough and segregation decreases but saturates to nonzero values.

C. Layering instability

Figure 9(a) shows the intermediate situation where partial segregation is observed. We obtain the azimuthal correlation function $g(\phi)$ of the particle density inside the pile to characterize the layering where $g(\phi)$ is given by

$$g(\phi) = \sum_{x,y,r_2} \frac{I(x,y)I(x+r_2 \cos(\phi), y+r_2 \sin(\phi))}{I(x,y)^2}, \quad (5)$$

where $I(x,y)$ is the particle ratio at position (x,y) and r_2 and ϕ define the distance from the point where correlation is calculated. The correlation function was calculated for a

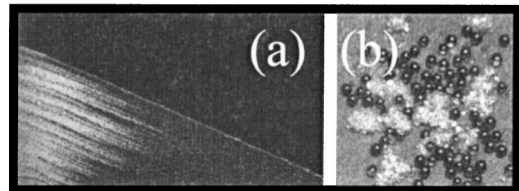


FIG. 9. (a) Strong layering is observed at V_f below V_c for $r=2.4$ (here, $V_f = 1.2 \times 10^{-3}$). (b) The fluid is observed to selectively coat the smaller particles, resulting in clumps of small particles. In this case, the clumps of small particles are larger than the larger particles.

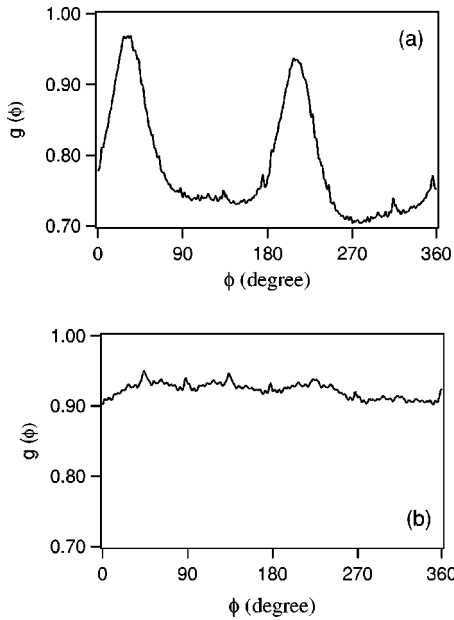


FIG. 10. Azimuthal correlation function of the density of the particles for (a) $V_f = 1.2 \times 10^{-3}$ and (b) $V_f = 6 \times 10^{-3}$. The correlation function shows two distinct peaks at the angles parallel to the surface. The peaks fade for higher V_f . The strongest layering is observed for $r = 2.4$.

square region in the middle of the pile. The peaks were observed to decrease in amplitude and are hidden by the noise if the whole pile was used for averaging. Figure 10(a) shows $g(\phi)$ for the image shown in Fig. 9(a). The correlation function has two distinct peaks corresponding to the angles parallel to the surface. The peaks are observed to decrease in amplitude as layering fades with increased V_f . Finally, for the complete mixture we observe the flat line shown in Fig. 10(b) for $V_f = 6 \times 10^{-3}$. The correlation function does not show peaks for larger size ratios consistent with the visual observation.

Although the layering is not as periodic as in *dry* mixtures of rough and smooth particles [12], some stratification is clearly observed below V_c . We believe that the layering is related to the selective coating and clumping of smaller particles (see Fig. 9). A clump of small particles effectively behaves as a particle with a rough surface that may be greater than the individual large particle. Makse *et al.* have shown that stratification may occur when two species with different surface roughness are present in granular flows when the size of the rough particles exceeds the smoother particles [12]. The features observed in Fig. 9 appear to be related to this mechanism, although the increased stick-slip nature of the flow at the surface brought about by the addition of the fluid makes the layering aperiodic. The strongest layering is observed for BD-2 and decreases at higher r where the clumps of small particles stay smaller than the larger beads. At higher V_f , the average size of clumps increases and the interaction between small and large particles also becomes important. Thus, clumps with small and large particles and layering disappears.

D. Viscosity dependence of the segregation

Next, we examine the effect of the viscosity of the fluid on the extent of segregation. As in the measurements for θ_r , we change the viscosity of the fluid by using mixtures of water and glycerol to keep the surface tension almost constant. s corresponding to water and glycerol is plotted in Fig. 8. The segregation is observed to decrease to zero at a lower value of V_f in the case of higher glycerol, which has ν a thousand times that of water. In fact, although some incipient amount of segregation is observed for large r in the case of water, segregation is observed to completely disappear in the case of glycerol for all measured r .

In Sec. III C, we discussed the strength of the viscous forces that may be important in determining percolation. For the particles ($d \sim 1.2$ mm) used in the experiments, and for glycerol or water as interstitial fluid, the saturation force due to surface tension is of the order of 10^{-4} N. Therefore, the viscous force is greater than the capillary force in the case of glycerol. The viscous force damps velocity fluctuation as it increases with relative velocity between particles. Because velocity fluctuations and percolation are required for segregation, s is therefore observed to be lower at higher ν for similar Γ . Since the linear increase of θ_r , and the decrease of s occurs below a similar V_c , and both of these quantities saturate above this volume fraction, the cohesion due to the fluid appears to have the same effect on both θ_r and s .

V. EXPERIMENTS WHEN PARTICLES ARE IMMERSSED IN THE FLUID

In this section, we study the angle of repose and the progress of segregation when the bidisperse glass particles are poured into a silo filled with various liquids with different ν . The procedure and the system is similar to the previous sections, except that in these experiments, we first fill the silo with the fluid and then pour the dry granular matter. In this case, only viscous forces are present and capillary forces are not present because liquid bridges are absent.

Because the terminal velocity for particles decreases with ν , they take a significantly longer time to drain in a viscous fluid compared to that in air and $Q < 0.02$ g s $^{-1}$ in glycerol. As ν is increased, the particles are increasingly observed to deviate from a downward trajectory and are deflected further down the slope even before coming in contact with the surface. The reason for the deflection of the particles may be qualitatively understood as follows. For a particle moving with velocity v , a boundary layer develops in the fluid that is proportional to $\sqrt{\nu d / \rho v}$. This estimate is essentially from dimensional arguments [22]. As the distance between the particle and the surface becomes comparable to the size of this boundary layer, the particles feel a net horizontal force similar to the viscous forces discussed earlier due to fluid expulsion. These forces tend to deflect the particles further down the slope.

We observed θ_r is $\sim 24^\circ \pm 1^\circ$ for mono and bidisperse glass particles for not only water and glycerol but also using polybutene (see Table II). Unlike the case of partial V_f , no systematic dependence of θ_r is observed on the viscosity.

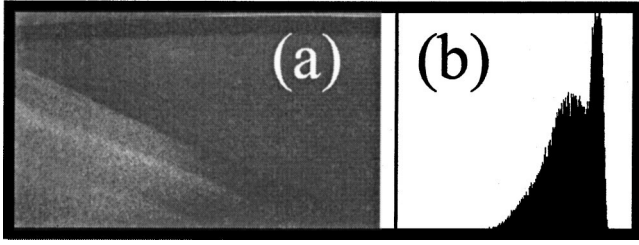


FIG. 11. Image of the granular pile after bidisperse glass beads ($r=2.4$) are poured into a silo filled with glycerol. Compare the extent of segregation to Fig. 6(a), where air is the interstitial medium. The segregation is drastically reduced when particles are poured into a more viscous medium. (b) The histogram of local particle density ratio of the two kinds of particles in the pile.

Furthermore, the observed θ_r in the fluid is very similar to that observed in air. This appears to suggest that the viscous forces discussed in Sec. III C may not be relevant in the absence of liquid bridges. Although it must be noted that the experiments conducted in the regime where the particles are mixed with a small volume fraction of fluid is somewhat different in nature than these experiments because of the presence of the boundary layer.

Experimental work investigating liquid bridges between moving spheres [18,23,24] has shown that bridge rupture distance and time between particles increases with viscosity. It is, therefore, possible that the increases in θ_r with viscosity in the case of partial V_f is related to the increase in the number and change in structure of liquid bridges with viscosity.

Figure 11(a) shows an image of the granular pile after bidisperse particles (BD-2) were poured into the silo filled with glycerol. Separate series of experiments to calibrate the intensity of light scattered by particles to the number of particles were first conducted when particles were completely immersed in the various fluids. Using the same procedure as before, we measured the histogram of light intensity to determine s [see Fig. 11(b)]. Comparing Fig. 11(a) to Fig. 6(a) shows a significant drop in s , when particles are poured in glycerol instead of air. The s is plotted in Fig. 12(a) as a function of ν for three different r . The segregation is observed to decrease as a function of ν and drops to zero at high ν which depends on r .

The observed decreases in segregation with ν may be explained as follows. The boundary layer washes away the details of the surface roughness of the pile at higher ν . Thus, the capture mechanism that is sensitive to surface roughness decreases in importance with ν . Furthermore, velocity fluctuations at higher ν are damped out as particles reach terminal velocity over a short distance leading to a reduction in percolation of particles [13]. Therefore, the segregation decreases because the two mechanisms that cause segregation in dry granular matter diminish in strength.

It is well known that sedimentation of different-sized particles (for example, in lakes) cause layering of different size particles to occur at the bottom because the terminal velocity reached by a spherical particle is proportional to \sqrt{d} . This does not occur in our geometry because particles are constantly fed into the system from the reservoir.

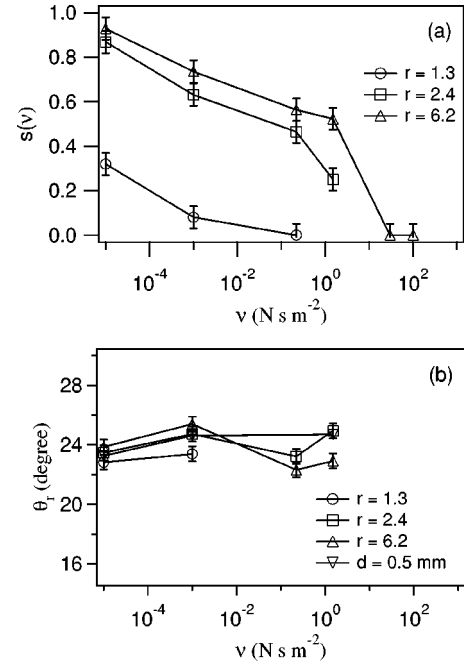


FIG. 12. (a) The extent of segregation $s(\nu)$ is observed to decrease as a function of ν of the fluid. (b) θ_r as a function ν is approximately constant. This is in contrast to observations for partial V_f where θ_r is observed to increase.

VI. CONCLUSIONS

In conclusion, the role of the size ratio of the particles, volume fraction, surface tension, and viscosity of the fluid on the extent of segregation and the angle of repose of a granular pile is clarified based on experiments and physical arguments. The angle of repose of the granular matter is observed to increase sharply as the volume fraction of the fluid is increased and then saturates. The saturation occurs at a higher V_f than estimated by using only particle roughness ideas. We observe that the viscosity of the fluid has a significant effect on the angle of repose of the pile. A sharp reduction of segregation is observed in the granular flow when a small volume fraction of fluid is added. The sharp changes in the angle of repose and segregation occurs over similar volume fractions, suggesting that cohesivity has the same effect on both properties. The experiments point to a need for examining the role of the number of liquid bridges between particles in determining the angle of repose. Our experiments appear to indicate that the changes in the number of liquid bridges and their structure with volume fraction, surface tension, and viscosity of the fluid may be very important in determining the properties of wet granular matter.

ACKNOWLEDGMENTS

We thank Jacob Goodman for help in acquiring data, and G. McKinley for bringing Ref. [18] to our attention. This work was supported by the National Science Foundation under Grant No. DMR-9983659, the Alfred P. Sloan Foundation, and by the donors of the Petroleum Research Fund.

- [1] H.M. Jaeger *et al.*, *Europhys. Lett.* **11**, 619 (1990).
- [2] A. Mehta, in *Granular Matter*, edited by A. Metha (Springer-Verlag, New York, 1993), p. 1.
- [3] R.M. Nedderman, *Statics and Kinematics of Granular Matter* (Cambridge University Press, Cambridge, 1992).
- [4] D.J. Hornbaker *et al.*, *Nature (London)* **387**, 765 (1997); R. Albert *et al.*, *Phys. Rev. E* **56**, 6271 (1997).
- [5] P. Tegzes *et al.*, *Phys. Rev. E* **60**, 5823 (1999).
- [6] T.G. Mason, A.J. Levine, D. Ertas, and T.C. Halsey, *Phys. Rev. E* **60**, R5044 (1999).
- [7] T.C. Halsey and A.J. Levine, *Phys. Rev. Lett.* **80**, 3141 (1998).
- [8] L. Bocquet, E. Charlaix, S. Ciliberto, and J. Crassous, *Nature (London)* **396**, 735 (1998).
- [9] N. Fraysse, H. Thome, and L. Petit, *Eur. Phys. J. B* **11**, 615 (1999).
- [10] J. Bridgwater, *Granular Matter*, edited by A. Metha (Springer-Verlag, New York, 1993), p. 161.
- [11] S. Savage and C.K.K. Lun, *J. Fluid Mech.* **189**, 311 (1988).
- [12] H.A. Makse, S. Halvin, P.R. King, and H.E. Stanley, *Nature (London)* **386**, 379 (1997).
- [13] J. Bridgwater and I. Tranter, *J. Powder Bulk Technol.* **2**, 9 (1978).
- [14] A. Samadani and A. Kudrolli, *Phys. Rev. Lett.* **85**, 5102 (2000).
- [15] A. Castellanos *et al.*, *Phys. Rev. Lett.* **82**, 1156 (1999).
- [16] A. Samadani, A. Pradhan, and A. Kudrolli, *Phys. Rev. E* **60**, 7203 (1999).
- [17] *Handbook of Chemistry and Physics*, 59th ed., edited by R.C. Weast (CRC Press, Boca Raton, FL, 1978).
- [18] O. Pitois, P. Moucheront, and X. Chateau, *J. Colloid Interface Sci.* **231**, 26 (2000).
- [19] Y. Xu, W. Huang, and G. Lian, in *Powders and Grains 2001*, edited by Y. Kihino (Balkema, Tokyo, 2001), p. 611.
- [20] B.J. Persson, *Sliding Friction* (Springer, New York, 1998), Chap. 7.
- [21] T. Boutreax and P.G. deGennes, *J. Phys. I* **6**, 1295 (1996).
- [22] G.K. Batchelor, *An Introduction to Fluid Dynamics* (Cambridge University Press, London, 1970).
- [23] S. Gaudet, G.H. McKinley, and H.A. Stone, *Phys. Fluids* **8**, 2568 (1996).
- [24] G. McKinley and A. Tripathi, *J. Rheol.* **44**, 653 (2000).